Int J Adv Manuf Technol (2011) 52:101–114
DOI 10.1007/s00170-010-2714-3

ORIGINAL ARTICLE

Performance comparison of conventional and wiper ceramic inserts in hard turning through artificial neural network modeling

Vinayak Neelakanth Gaitonde · S. R. Karnik · Luis Figueira · J. Paulo Davim

Received: 12 September 2009 / Accepted: 3 May 2010 / Published online: 19 May 2010

Abstract Hard turning with ceramic tools provides an alternative to grinding operation in machining high precision and hardened components. But, the main concerns are the cost of expensive tool materials and the effect of the process on machinability. The poor selection of cutting conditions may lead to excessive tool wear and increased surface roughness of workpiece. Hence, there is a need to investigate the effects of process parameters on machinability characteristics in hard turning. In this work, the influence of cutting speed, feed rate, and machining time on machinability aspects such as specific cutting force, surface roughness, and tool wear in AISI D2 cold work tool steel hard turning with three different ceramic inserts, namely, CC650, CC650WG, and GC6050WH has been studied. A multilayer feed-forward artificial neural network (ANN), trained using error back-propagation training algorithm has been employed for predicting the machinability. The input–output patterns required for ANN training and testing are obtained from the turning experiments planned through full factorial design. The simulation results demonstrate the effectiveness of ANN models to analyze the effects of cutting conditions as well as to study the performance of conventional and wiper ceramic inserts on machinability.

Keywords Hard turning · High chromium AISI D2 cold work tool steel · Conventional and wiper ceramic inserts · Machinability · Artificial neural network

V. N. Gaitonde (✉)
Department of Industrial and Production Engineering, B. V. B. College of Engineering and Technology,
Hubli 580 031 Karnataka, India
e-mail: gaitondevn@yahoo.co.in

S. R. Karnik
Department of Electrical and Electronics Engineering, B. V. B. College of Engineering and Technology,
Hubli 580 031 Karnataka, India
e-mail: karniksr@yahoo.com

L. Figueira · J. P. Davim
Department of Mechanical Engineering, University of Aveiro,
Campus Santiago,
3810-193 Aveiro, Portugal

L. Figueira
e-mail: lfigueira@mec.ua.pt

J. P. Davim
e-mail: pdavim@ua.pt

1 Introduction

The machining of hardened steel components (45-65 HRC) has been extensively used to replace the grinding operations due to improvements in the performance of hard tool materials such as ceramics and cubic boron nitride (CBN). The possibility of eliminating coolant reduced processing costs and power consumption, improved material properties and productivity, flexibility in producing complex geometric errors, ability to machine thin wall sections, and comparable surface finish are the major benefits of hard turning [1, 2]. Hence, hard turning is broadly used in many applications such as tools, dies, gears, cams, shafts, axles, and bearings [3–6].

The hard turning can provide a reasonably high accuracy for the hardened components, but the important problems occur with surface finish and tool wear [7, 8]. The generation of undesirable residual stresses and the formation of tempered white and dark layers in machined surfaces affect the surface quality of the hardened component [9, 10]. Moreover, the cutting tools employed for hard turning are relatively costly compared with grinding, and hence, there is a need to investigate the tool life.

Furthermore, it has been reported that the properties and composition of cutting tool materials are crucial to the behavior of machining forces, which in turn affect the surface finish and tool life [11]. Therefore, it is essential to study the effects of machining parameters on hard turning process.

Chou and Evans [12], Chou et al. [13], Thiele and Melkote [14], and Ozel et al. [15] evaluated the performance of CBN cutting tool in terms of cutting forces, surface roughness, tool wear, and surface integrity during hard turning of different grades of steels. The tool wear behavior and surface integrity in high-speed turning of hardened steel with polycrystalline cubic boron nitride tools was studied by Kishawy and Elbestawi [16]. The effects of cutting conditions and tool wear on chip morphology, quality, and surface integrity of machined surfaces during AISI D2 tool steel hard turning was observed by El-Wardany et al. [17, 18]. Poulachon et al. [19] noted the influence of microstructure of hardened steel components on tool wear mechanisms. Lima et al. [20] published the results of an investigation concerning the effect of cutting speed, feed rate and depth of cut on cutting forces, tool wear, and surface roughness in hardened AISI 4340 high strength low alloy steel and AISI D2 cold work tool steel materials. Pavel et al. [21] analyzed the tool wear behavior on surface finish in interrupted and continuous hard turning. Diniz and Oliveira [22] found the best tool material and tool cutting edge micro-geometry for turning continuous, semi-interrupted, and interrupted surfaces of AISI 4340 hardened steel in terms of tool wear and tool life.

The investigative study carried out by Chou and Song [23] reveals that a large tool nose radius can provide better surface finish but generates deeper white layers in AISI 52100 bearing steel turning using alumina titanium-carbide tools. Kumar et al. [24] and Benga and Abrao [25] employed alumina–TiC ceramic tools in turning of hardened steel components and observed a good surface finish. Grzesik and Wanat [26] presented a comprehensive analysis of part surface finish in continuous dry turning of hardened construction steel with mixed alumina cutting tools. Furthermore, Grzesik and Wanat [27] described the surface roughness characteristics during turning of hardened low chromium alloy steel using mixed alumina–titanium carbon (TiC) ceramic cutting tools equipped with both conventional and wiper inserts. Later, Grzesik [28] also reported the characterization of surface roughness during hard turning with conventional as well as wiper ceramic cutting tools at variable feed rates. Schwach and Guo [29] focused their study on surface topography, surface roughness, micro-hardness, subsurface microstructure, and residual stresses during turning of AISI 52100 components.

Quiza et al. [30] developed the statistical and artificial neural network (ANN) models for predicting the tool wear in hard turning of AISI D2 steel using conventional ceramic inserts. Ozel and Karpat [31] also proposed the regression and ANN models for predicting the surface roughness and tool wear during hard turning of AISI H13 steel with CBN inserts. Davim and Figueira [32] performed statistical analysis to study the influence of cutting speed and feed rate on flank wear, specific cutting pressure, and surface roughness in hard turning of AISI D2 cold work tool steel with conventional ceramic inserts. Recently, the wiper ceramic inset has been introduced for the substantial improvement of surface finish in machining of hardened components [33–36].

A review of literature cited above clearly indicates that, even though a large number of research works have been reported in the area of hard turning, the performance comparison of conventional and wiper ceramic inserts in terms of machinability has not been studied during hard turning of AISI D2 cold work tool steel. AISI D2 cold work tool steel is one of the important hardened steels used for many types of tools and dies and other applications where high wear resistance and low costs are of prime importance. Keeping this consideration in view, an attempt has been in this paper to predict the machinability aspects such as specific cutting force in operation, surface roughness in workpiece, and tool wear in cutting tool during hard turning process.

The model development by response surface methodology (RSM) is a convenient method that requires minimum number of experiments, thus reducing the cost and time [37]. However, RSM based mathematical models are restricted to only small range of input parameters and hence are not suitable for highly complex and non-linear processes. Hence, a multilayer feed-forward back-propagation ANN has been

Table 1 Identified process parameters and their levels

Process parameter	Symbol	Unit	Level		
			1	2	3
Ceramic insert	I	–	CC650	CC650WG	GC6050WH
Cutting speed	v	m/min	80	115	150
Feed rate	f	mm/rev	0.05	0.1	0.15
Machining time	t	min	5	10	15

Table 2 Experimental layout plan and the experimental results

Trial no.	Settings of process parameters				Machinability characteristics		
	I	*v* (m/min)	*f* (mm/rev)	*t* (min)	K_s (MPa)	R_a (microns)	*VC* (mm)
Training patterns							
1	CC650	80	0.05	5	3,719.11	0.16	0.032
2	CC650	80	0.05	10	6,491.41	0.33	0.068
3	CC650	80	0.1	5	3,951.91	0.39	0.086
4	CC650	80	0.1	15	6,667.59	0.57	0.190
5	CC650	80	0.15	10	5,033.12	1.46	0.148
6	CC650	80	0.15	15	5,178.99	1.33	0.156
7	CC650	115	0.05	5	8,017.18	0.31	0.081
8	CC650	115	0.05	15	9,315.76	0.43	0.146
9	CC650	115	0.1	5	5,489.32	0.87	0.102
10	CC650	115	0.1	10	5,474.35	1.07	0.131
11	CC650	115	0.15	10	4,568.57	1.12	0.111
12	CC650	115	0.15	15	4,683.02	1.31	0.152
13	CC650	150	0.05	10	8,081.68	0.34	0.137
14	CC650	150	0.05	15	8,138.2	0.53	0.179
15	CC650	150	0.1	5	5,172.06	0.49	0.085
16	CC650	150	0.1	15	5,916.48	1.09	0.242
17	CC650	150	0.15	5	4,266.36	1.04	0.144
18	CC650	150	0.15	10	5,633.37	0.82	0.262
19	CC650WG	80	0.05	10	7,160.19	0.26	0.083
20	CC650WG	80	0.05	15	8,739.71	0.23	0.089
21	CC650WG	80	0.1	5	4,884.21	0.17	0.053
22	CC650WG	80	0.1	15	7,308.82	0.26	0.113
23	CC650WG	80	0.15	5	6,106.92	0.29	0.106
24	CC650WG	80	0.15	10	6,360.56	0.42	0.138
25	CC650WG	115	0.05	5	9,370.5	0.31	0.106
26	CC650WG	115	0.05	15	9,503.99	0.31	0.164
27	CC650WG	115	0.1	10	5,982.98	0.49	0.142
28	CC650WG	115	0.1	15	5,976.39	0.54	0.186
29	CC650WG	115	0.15	5	5,049.41	0.38	0.099
30	CC650WG	115	0.15	10	5,012.96	0.54	0.122
31	CC650WG	150	0.05	10	8,605.74	0.14	0.127
32	CC650WG	150	0.05	15	9,728.38	0.18	0.168
33	CC650WG	150	0.1	5	6,728.23	0.23	0.095
34	CC650WG	150	0.1	15	7,477.71	0.3	0.245
35	CC650WG	150	0.15	5	4,792.78	0.49	0.115
36	CC650WG	150	0.15	10	4,742.27	0.71	0.170
37	GC6050WH	80	0.05	5	6,207.86	0.25	0.047
38	GC6050WH	80	0.05	10	9,316.2	0.34	0.07
39	GC6050WH	80	0.1	5	6,803.49	0.53	0.077
40	GC6050WH	80	0.1	15	7,218.18	0.55	0.164
41	GC6050WH	80	0.15	10	6,051.85	0.74	0.111
42	GC6050WH	80	0.15	15	5,558.97	0.61	0.143
43	GC6050WH	115	0.05	5	8,256.18	0.2	0.071
44	GC6050WH	115	0.05	10	8,331.79	0.21	0.091
45	GC6050WH	115	0.1	5	5,802.83	0.24	0.076
46	GC6050WH	115	0.1	15	5,669.92	0.5	0.151

Table 2 (continued)

Trial no.	Settings of process parameters				Machinability characteristics		
	I	*v* (m/min)	*f* (mm/rev)	*t* (min)	K_s (MPa)	R_a (microns)	*VC* (mm)
47	GC6050WH	115	0.15	10	4,752.68	0.5	0.112
48	GC6050WH	115	0.15	15	5,588.35	0.59	0.133
49	GC6050WH	150	0.05	5	6,645.78	0.18	0.074
50	GC6050WH	150	0.05	10	7,012.23	0.2	0.098
51	GC6050WH	150	0.1	10	6,122.5	0.43	0.106
52	GC6050WH	150	0.1	15	6,343.75	0.62	0.144
53	GC6050WH	150	0.15	5	5,012.38	0.46	0.081
54	GC6050WH	150	0.15	15	5,165.32	0.7	0.158
Testing patterns							
1	CC650	80	0.05	15	8,008.64	0.53	0.112
2	CC650	80	0.1	10	6,149.04	0.52	0.134
3	CC650	80	0.15	5	3,818.14	1.32	0.089
4	CC650	115	0.05	10	8,336.07	0.29	0.097
5	CC650	115	0.1	15	5,770.13	1.06	0.177
6	CC650	115	0.15	5	4,402.13	1.28	0.09
7	CC650	150	0.05	5	6,999.36	0.37	0.104
8	CC650	150	0.1	10	5,509.53	0.72	0.151
9	CC650	150	0.15	15	5,783.37	1.24	0.333
10	CC650WG	80	0.05	5	4,128.03	0.18	0.052
11	CC650WG	80	0.1	10	6,299.24	0.23	0.083
12	CC650WG	80	0.15	15	6,793.39	0.48	0.164
13	CC650WG	115	0.05	10	9,185.2	0.35	0.141
14	CC650WG	115	0.1	5	6,028.54	0.39	0.096
15	CC650WG	115	0.15	15	4,944.25	0.55	0.140
16	CC650WG	150	0.05	5	8,313.24	0.16	0.095
17	CC650WG	150	0.1	10	7,663.66	0.24	0.176
18	CC650WG	150	0.15	15	5,732.94	0.91	0.233
19	GC6050WH	80	0.05	15	9,706.24	0.52	0.086
20	GC6050WH	80	0.1	10	6,876.04	0.57	0.111
21	GC6050WH	80	0.15	5	5,929.33	0.61	0.067
22	GC6050WH	115	0.1	10	5,836.78	0.36	0.104
23	GC6050WH	115	0.15	5	4,944.05	0.35	0.077
24	GC6050WH	115	0.05	15	8,834.84	0.25	0.111
25	GC6050WH	150	0.05	15	8,432.31	0.21	0.148
26	GC6050WH	150	0.1	5	5,784.38	0.28	0.083
27	GC6050WH	150	0.15	10	5,168.53	0.69	0.120

employed in this work to establish the relationship between the process parameters such as tool material, cutting speed, feed rate, and machining time on machinability characteristics. The input–output data required to develop the ANN model has been obtained through turning experiments based on full factorial design (FFD). The ANN is found to be an efficient modeling tool and has been applied in the recent past for several machining processes [38–41].

2 Artificial neural network modeling

The neural networks are highly flexible modeling tools with an aptitude to learn the mapping between input and output parameters [42, 43]. The purpose of ANN development is to imitate human brain so as to implement the functions such as association, self-organization, and generalization. The ANNs are parallel computer models of processes and

Table 3 Chemical composition of high chromium AISI D2 cold work tool steel material (wt %)

Cr	C	V	Mo	Mn	Si
11.80	1.55	0.8	0.8	0.40	0.30

the mechanisms that constitute biological nerve systems. In addition to adaptive nature and capability in solving complex and non-linear problems, ANNs are attractive in view of their high execution speed and modest computer hardware requirements. The ANN is made up of neurons connected together via links. The information is processed within the neurons and is propagated to other neurons through the links connecting the neurons.

In the current research, a feed-forward ANN using error back-propagation training algorithm (EBPTA) has been employed. The EBPTA is a supervised learning algorithm based on generalized delta rule [42, 43], which requires a set of inputs and desired outputs, known as training patterns. The EBPTA uses a gradient search technique that updates the synaptic weights during the learning stage in such a way that mean square error between actual output pattern of network and desired output pattern is minimized.

The multilayer feed-forward ANN consists of neurons divided into input layer, hidden layers, and output layer. The net activation input for ith neuron is given by [42]:

$$net_i = \sum_{j=1}^{n} w_{ij} x_j \tag{1}$$

where, w_{ij}=weight of link connecting neuron i to j; x_j= the output of jth neuron. For an unipolar sigmoid transfer function, the ouput of ith neuron is given as [42]:

$$o_i = \frac{1}{1 + e^{\eta net_i}} \tag{2}$$

where, η is the scaling factor. The training algorithm adapted here is based on the weight updates so as to minimize the sum of squared error for K number of neurons in the output layer and is given by:

$$E = \frac{1}{2} \sum_{k=1}^{K} \left(d_{k,p} - o_{k,p}\right)^2 \tag{3}$$

where, $d_{k,p}$=desired output for pth pattern. The synaptic weights of the links are updated as:

$$w_{ji(n+1)} = w_{ji(n)} + \alpha \delta_{pj} o_{pi} + \beta \Delta w_{ji(n)} \tag{4}$$

where, n is the learning step, α is the learning rate, and β is the momentum constant. The error term δ_{pj} in Eq. 4 is given by:

- For output layer:

$$\delta_{pk} = \left(d_{kp} - o_{kp}\right)\left(1 - o_{kp}\right); k = 1, \ldots K \tag{5}$$

- For hidden layer:

$$\delta_{pj} = o_{pj}\left(1 - o_{pj}\right) \sum \delta_{pk} w_{kj}; j = 1, \ldots J \tag{6}$$

where, J is the number of neurons in the hidden layer.

The steps in ANN training using EBPTA are as follows:

1. The network weights are initialized to small random values.
2. The input/desired output pairs are presented one by one, updating the weights each time.
3. The mean square error (*MSE*) due to all outputs and *NP* number of patterns is computed as:

$$MSE = \frac{1}{NP} \sum_{p=1}^{NP} \sum_{k=1}^{K} \left(d_{kp} - o_{kp}\right)^2 \tag{7}$$

4. If (*MSE*<specified tolerance) or (epochs>$(\text{epochs})_{\max}$)

   Then stop.

   Else, goto step 2.

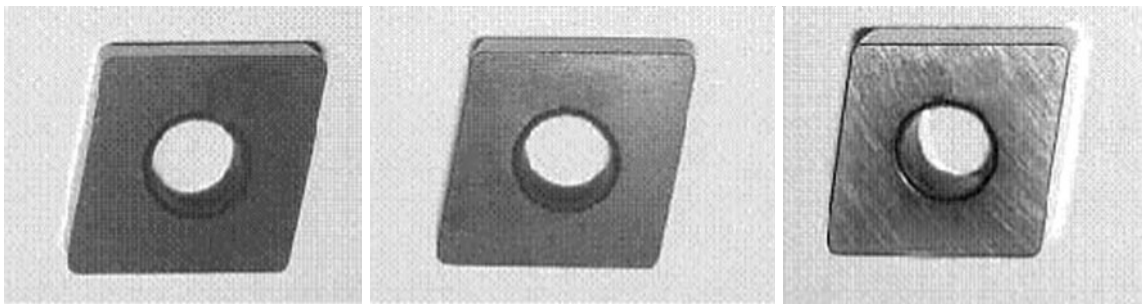

a) CC650 b) CC650WG c) GC6050WH

Fig. 1 Ceramic inserts employed in the experimentation

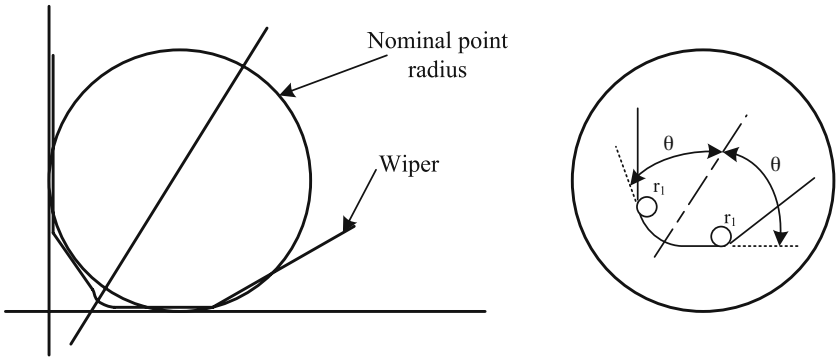

Fig. 2 Wiper geometry of ceramic insert used

3 Experimental details

3.1 Experimental planning

The database for the ANN model development is obtained through turning experiments. For building the experimental database, huge number of experiments is to be performed, which is time-consuming and costly. As the traditional experimental design methods are too complex, an experimental layout plan based on design of experiments [37] has been selected. In the present investigation, tool material, cutting speed, feed rate, and machining time are selected as the process parameters. Three ceramic inserts such as conventional CC650 and wiper ceramic inserts, namely CC650WG and GC6050WH, are selected as the cutting tool materials. Three levels for each of machining parameters such as cutting speed, feed rate, and machining time are identified. The ranges of these factors were selected based on the authors' previous investigations. The machining parameters considered and their levels identified are listed in Table 1. Table 2 presents the experimental layout plan as per FFD, which consists of 3^4 (=81) sets of process parameter combinations.

3.2 Experimentation

The present study was carried out with a high chromium AISI D2 cold work tool steel work bars. The chemical composition of the work material is in given in Table 3. The hardness of about 59-61 HRC was maintained through a quenching process in a vacuum atmosphere of 1,000–1,040°C.

Three different types of ceramic inserts such as conventional CC650 and wiper (multiple-point radii) of CC650WG and GC6050WH were used in the present investigation and are shown in Fig. 1. The mixed alumina insert with TiN coating [ISO code of *CNGA 120408T01020 WG*] has a chemical composition of Al_2O_3 (70%) and TiC (30%). It is obviously known that hard machining requires a negative rake angle, hence ceramic inserts with the following geometry has been employed: rake angle, −6º; clearance angle, 6º; major cutting edge angle, 95º; and cutting edge inclination angle, −6º. The tool holder of type "*DCLNL2020K12*" (ISO) was used throughout the research work. Figure 2 depicts the wiper geometry of the ceramic insert employed.

The machine used for turning tests is a high rigidity CNC lathe of type "*Kingsbury MHP 50*", equipped with

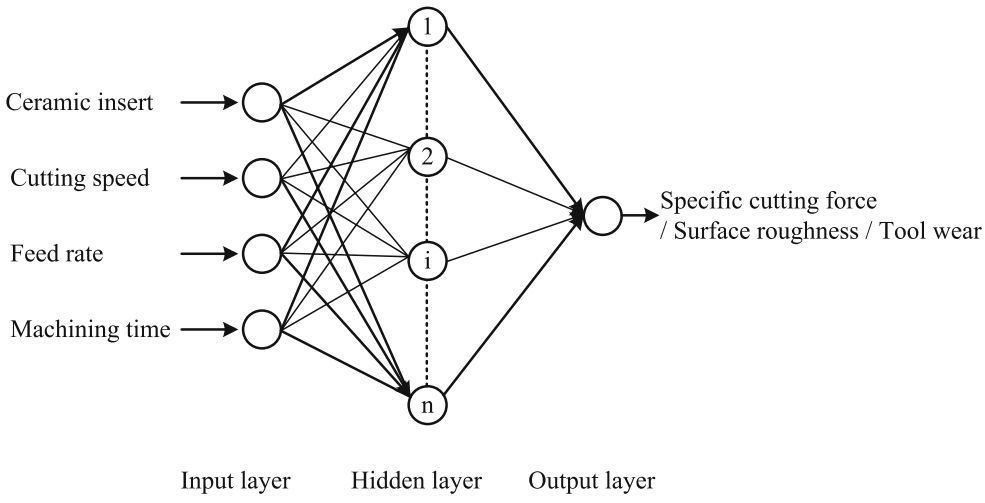

Fig. 3 Feed-forward ANN structure

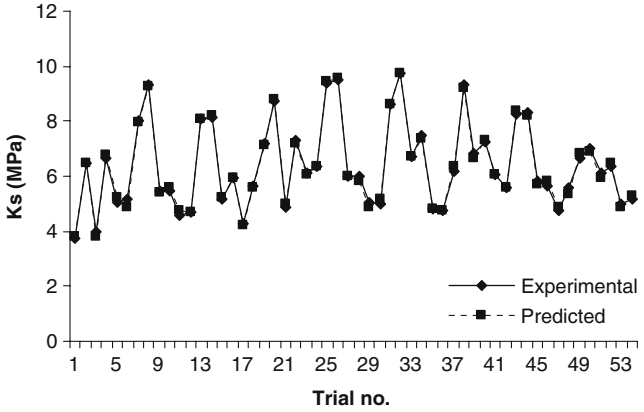

Fig. 4 Comparison of experimental and ANN predicted values of specific cutting force for training patterns

18 kW spindle power and maximum spindle speed of 4,500 rpm. The depth of cut of 0.2 mm was kept constant throughout the investigation. The experiments as per FFD were performed, and the trials were randomized.

3.3 Machinability evaluation

The cutting force (F_c) was measured through a 9121 model "*Kistler*®" piezoelectric dynamometer. The values were continuously monitored and recorded through a 5019-model charge amplifier with data acquisition.

The profilometer of type "*Hommelwerke® T1000*"was employed to measure the surface roughness on the machining surfaces, with a cut off of 0.8 mm in accordance to ISO/DIS 4287/1E. Each surface roughness measurement was replicated thrice, and the mean was taken as the arithmetic average surface roughness (R_a).

The "*Mitutoyo® TM-500*" tool makers' microscope with 30× magnification, and 1 μm resolution was used to evaluate flank tool wear. The admissible wear was established according to ISO 3685 standard (1993) and measured at corner radius (VB_C). Due to lower depth of cut

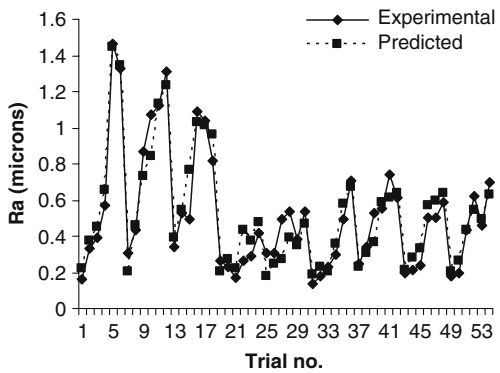

Fig. 5 Comparison of experimental and ANN predicted values of surface roughness for training patterns

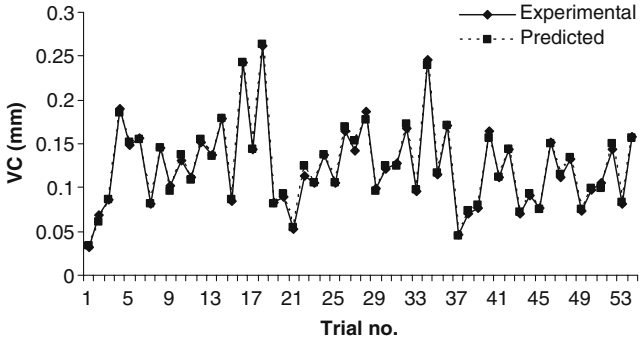

Fig. 6 Comparison of experimental and ANN predicted values of tool wear for training patterns

as compared with tool nose radius of 0.8 mm, VB_C is used instead of VB_B.

The specific cutting force (K_s) is determined as follows:

$$K_s = \frac{F_c}{f \times d} \tag{8}$$

where, d is the depth of cut. The computed values of specific cutting force (K_s) and the measured values of arithmetic surface roughness (R_a) and tool wear (VC) are summarized in Table 2.

4 Results and discussion

4.1 ANN training

The experimental results as shown in Table 2 were utilized for ANN modeling. The data set consists 81 patterns, of which the first 54 patterns (Table 2, "Training patterns") were utilized for training the network, and the last 27 patterns (Table 2, "Testing patterns") were selected for testing the performance of trained network. All the inputs and the desired outputs were normalized using the equation:

$$X_{\text{normal}} = \frac{2(X - X_{\min})}{(X_{\max} - X_{\min})} - 1 \tag{9}$$

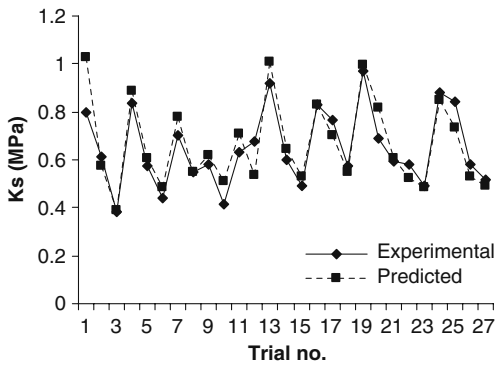

Fig. 7 Comparison of experimental and ANN predicted values of specific cutting force for validation data

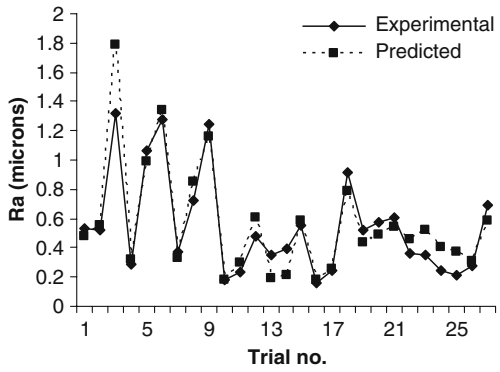

Fig. 8 Comparison of experimental and ANN predicted values of surface roughness for validation data

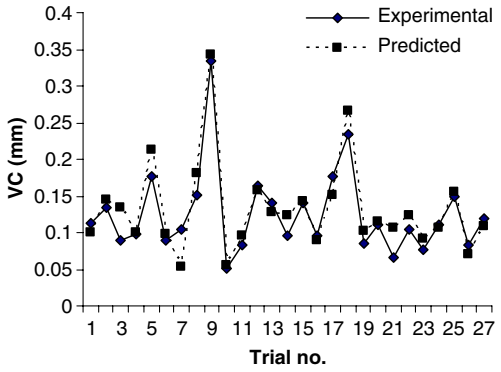

Fig. 9 Comparison of experimental and ANN predicted values of tool wear for validation data

where, X_{min}=minimum value in the vector of pattern for *X;* X_{max}=maximum value in the vector of pattern for *X.* This normalization maps all the inputs and desired outputs between –1 and +1. The ANN training for these 81 normalized input–output patterns has been carried out using *NN* tool box of MATLAB software [44].

The ANN training is sensitive to many factors such as number of neurons in hidden layers and the learning parameters [42]. The number of hidden neurons depends on input vector size and the number of classifications of input–output vector space. Too many neurons can lead to over-fitting, whereas few neurons can lead to under fitting, in which all the training points are well fit, but the fitting curve takes wild oscillations between these points. It was also found that the ANN has tendency to lose generalization in case of prolonged training beyond certain limits in an attempt to minimize MSE. Thus, the number of neurons in the hidden layers as well as learning parameters is to be determined by trial and error method and repeated training simulation.

A feed-forward ANN architecture for the present investigation is presented in Fig. 3. Three separate ANN models of specific cutting force, surface roughness, and tool wear developed. The ANN structure consists of four neurons in the input layer (corresponding to four machining parameters) and one neuron in the output layer (corresponding to one output). As suggested by Fausett [43], the back-propagation architecture with one hidden layer is enough for majority of the applications, and hence, a single hidden layer has been employed in the current investigation.

The ANN training simulation was performed using a variable learning rate training procedure "*traingdx*" of MATLAB NN toolbox [44]. Appropriate learning rate parameters for faster convergence and momentum factor for increasing the rate of learning have been selected. The training has been continued until MSE reaches 10^{-5} or 5,000 epochs. In the current study, after successful training, 4-8-1 architecture for specific cutting force model with a learning rate of 0.1; 4-4-1 and 4-10-1 structures for surface roughness and tool wear models with a learning rate of 0.05 were found to be suitable. The momentum constant of 0.95 and learning rate increment of 1.05 was found to be satisfactory for all the networks.

4.2 ANN testing

The ANN was initially tested with 54 input training patterns. For each input pattern, the experimental values of specific cutting force, surface roughness, and tool wear were compared with the respective predicted values. The percentage prediction accuracy of the developed model is given by:

$$\delta = \frac{100}{n}\sum_{i=1}^{n}\left|\frac{\left(y_{i,\exp t} - y_{i,\text{pred}}\right)}{y_{i,\text{pred}}}\right| \tag{10}$$

where, $y_{i,expt}$=experimental value of desired machinability for *i*th trial; $y_{i,pred}$=predicted value of desired machinability for *i*th trial and *n* is the number of trials. Figures 4, 5, and 6 display the comparison of the experimental values with the ANN predicted values for specific cutting force, surface roughness, and tool wear, respectively. The δ was found to be 1.59%, 18.47%, and 2.57% for specific cutting force, surface roughness, and tool wear, respectively.

The testing of the trained ANN was then performed with the remaining 27 trials of FFD, which were different from

Table 4 *R* values for developed machinability models

Machinability characteristic	*R* value	
	Training data	Validation data
Specific cutting force	0.997	0.906
Surface roughness	0.957	0.939
Tool wear	0.997	0.939

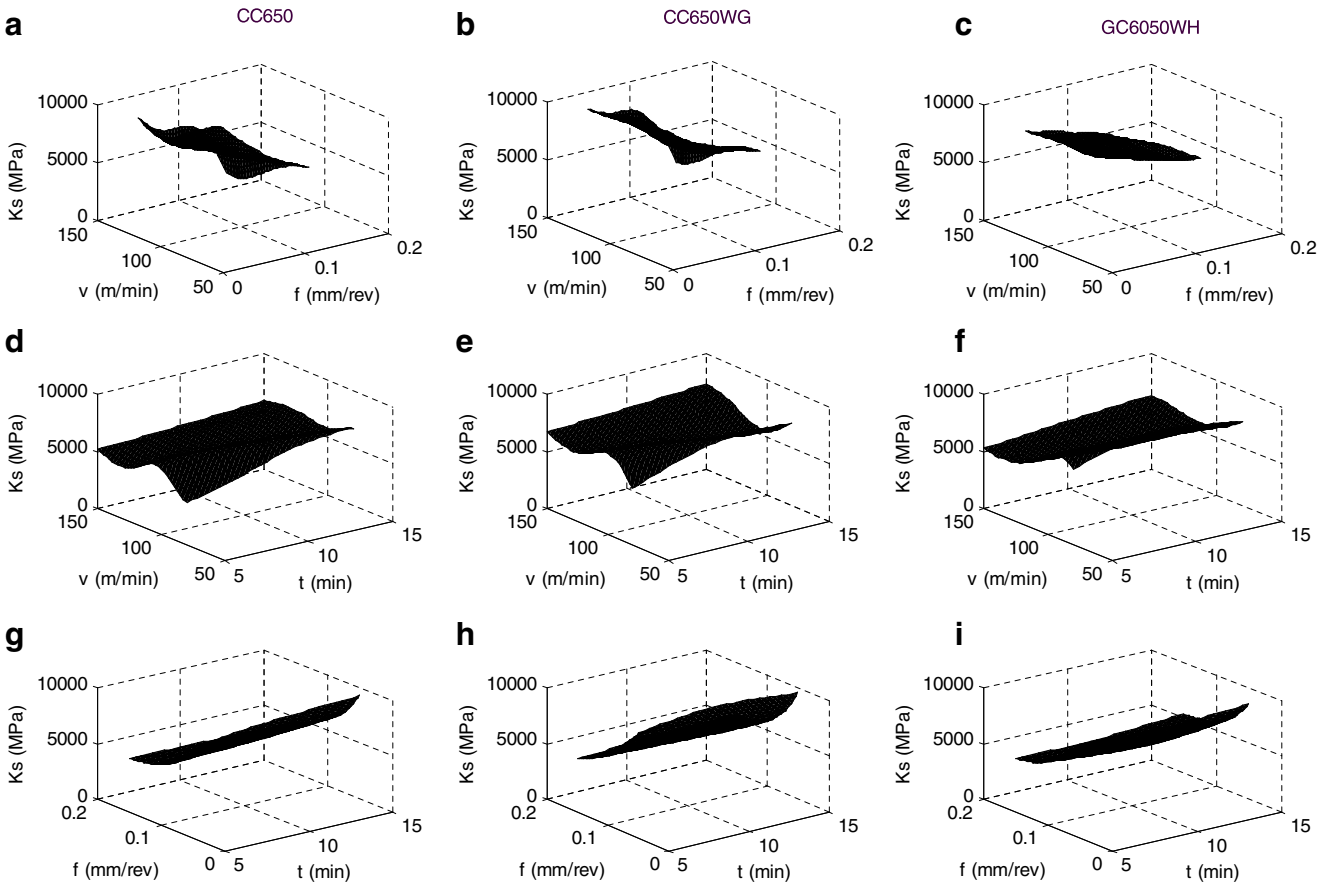

Fig. 10 Response surface plots showing the effect of two variables on specific cutting force: **a**–**c** cutting speed and feed rate; **d**–**f** Cutting speed and machining time; **g**–**i** feed rate and machining time

those used for training the network. The comparison of the the experimental with the ANN predicted values for specific cutting force, surface roughness, and tool wear for the validation data are presented in Figs. 7, 8, and 9, respectively. From these figures, it is clearly seen that the predicted values almost follow the same trend as that of the corresponding experimental values. For the validation data, the values of δ were found to be 8.39%, 20.57%, and 15.32% for specific cutting force, surface roughness, and tool wear, respectively.

Even though the performance of a trained network is measured to some extent by the errors on training, validation, and test sets, it is often useful to investigate the network output by performing a regression analysis between the output and the corresponding targets. This was carried out using the "*postreg*" in the MATLAB NN toolbox [44]. The correlation coefficient (R) between the outputs and targets is a measure of how well the variation in the output is explained by the targets. If R is 1, then it indicates the perfect correlation between the targets and the outputs. Table 4 illustrates the R value for the training patterns as well as the validation data, which clearly indicates a very good correlation.

4.3 Performance study of ceramic inserts on machinability

The two-factor interaction effects due to cutting speed (v)–feed rate (f), cutting speed (v)–machining time (t), and feed rate (f)–machining time (t) on specific cutting force (K_s), surface roughness (R_a) and tool wear (VC) during hard turning of AISI D2 cold work tool steel were analyzed for three different ceramic inserts, namely CC650, CC650WG, and GC6050WH through surface plots (Figs. 10, 11, and 12). The 3D response surface plots were generated considering two machining parameters at a time, while the other parameter was kept at the center level.

Figure 10a–c depicts the interaction effects of v and f on K_s during hard turning of cold work tool steel using three different ceramic inserts. It is observed that the behavior of K_s is highly non-linear with respect to both v and f in case of CC650 and CC650WG inserts. On the other hand, with GC6050WH, the behavior K_s is almost linear. However, in all the three inserts tested, minimum K_s results with higher f and lower v. A comparison shows that the GC6050WH wiper ceramic insert seems to be better, as it results in lower K_s values as compared with conventional CC650 and wiper CC650WG inserts.

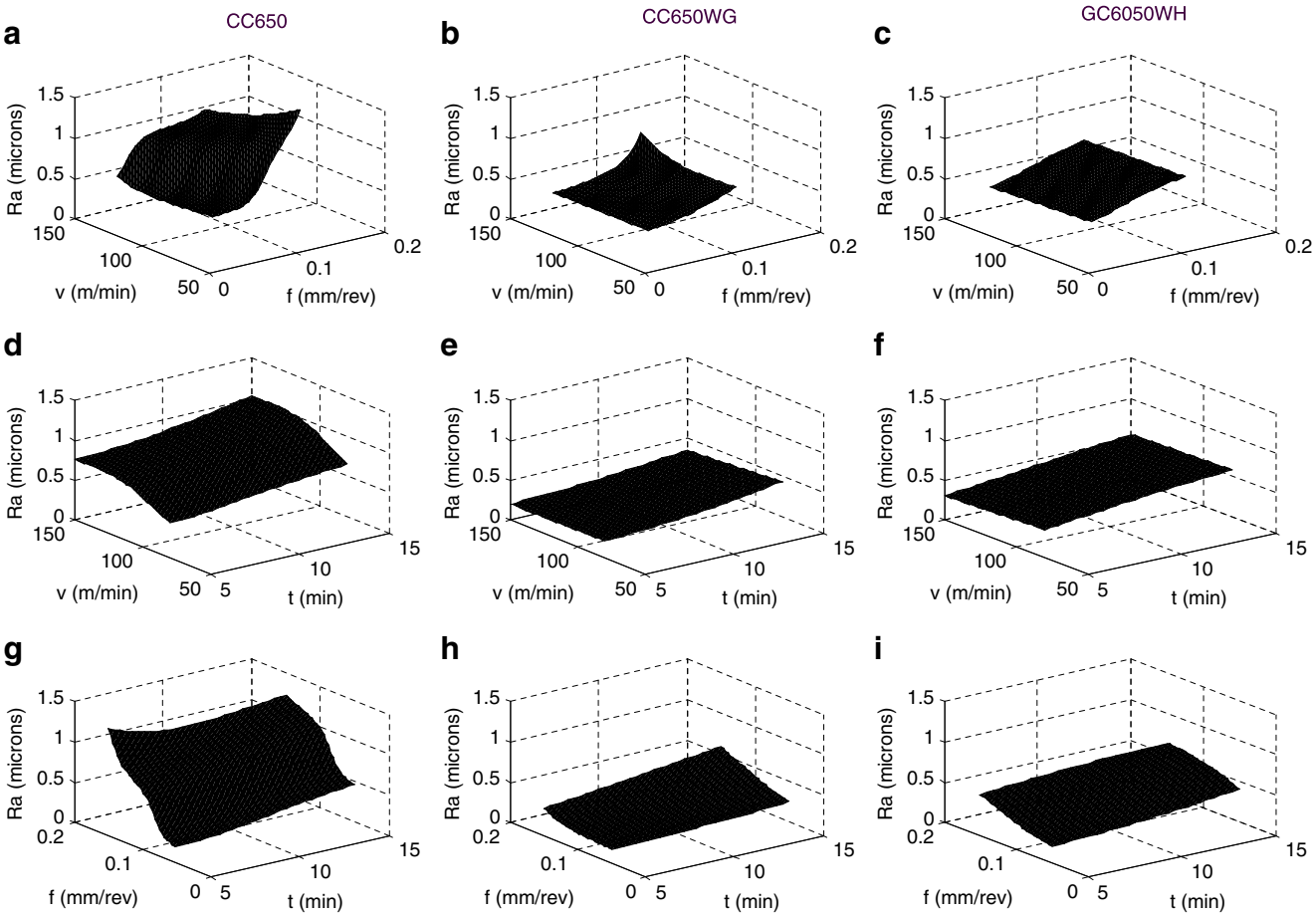

Fig. 11 Response surface plots showing the effect of two variables on surface roughness: **a**–**c** cutting speed and feed rate; **d**–**f** cutting speed and machining time; **g**–**i** feed rate and machining time

The estimated response surface for K_s in relation to v and t is shown in Fig. 10d–f. As seen from these figures, the behavior of K_s with respect to v and t is non-linear and more or less the same. It is observed that the minimal K_s results in lower values of both v and t for all the ceramic inserts tested. However, the comparison reveals that the K_s is more in case of CC650WG as compared with other inserts.

The variation of f and t on K_s with ceramic tool machining is exhibited in Fig. 10g–i. It is seen that, for a given f, K_s exhibits non-linear behavior and almost insensitive to t variations. Furthermore, it is observed that the wiper GC6050WH ceramic insert gives lesser K_s for specified values of f and t. Moreover, higher f values are necessary to minimize the K_s.

From the above, it is revealed that a combination of lower values of cutting speed and machining time along with higher feed rate values is necessary for minimizing the specific cutting force for all the three ceramic inserts tested. The GC6050WH ceramic insert performs better as compared with other inserts as far as specific cutting force is concerned.

The surface plots showing two-factor interaction effects of process parameters on R_a are presented in Fig. 11. It is clearly evidenced from these figures that the R_a is almost linearly related to the process parameters v, f, and t. The R_a is minimal, when all the three parameters are at lower levels for all the three ceramic inserts tested. A comparison graph indicates that both the wiper ceramic inserts CC650WG and GC6050WH results in minimal surface roughness as compared with conventional CC650.

Figure 12 illustrates the two-factor effects of machining parameters on VC. The tool wear is highly sensitive to v and f as compared with t for all the ceramic inserts. Moreover, the tool wear increases with the increase in any one of the process parameters v, f, and t. This clearly suggests that the tool wear can be minimized by employing lower values of v, f, and t. Furthermore, it is also observed that GC6050WH wiper ceramic insert is preferable than the other two inserts, as it provides lesser tool wear.

From the above discussions, it can be concluded that the machinability performance in terms of specific cutting force and tool wear, the GC6050WH wiper ceramic insert is

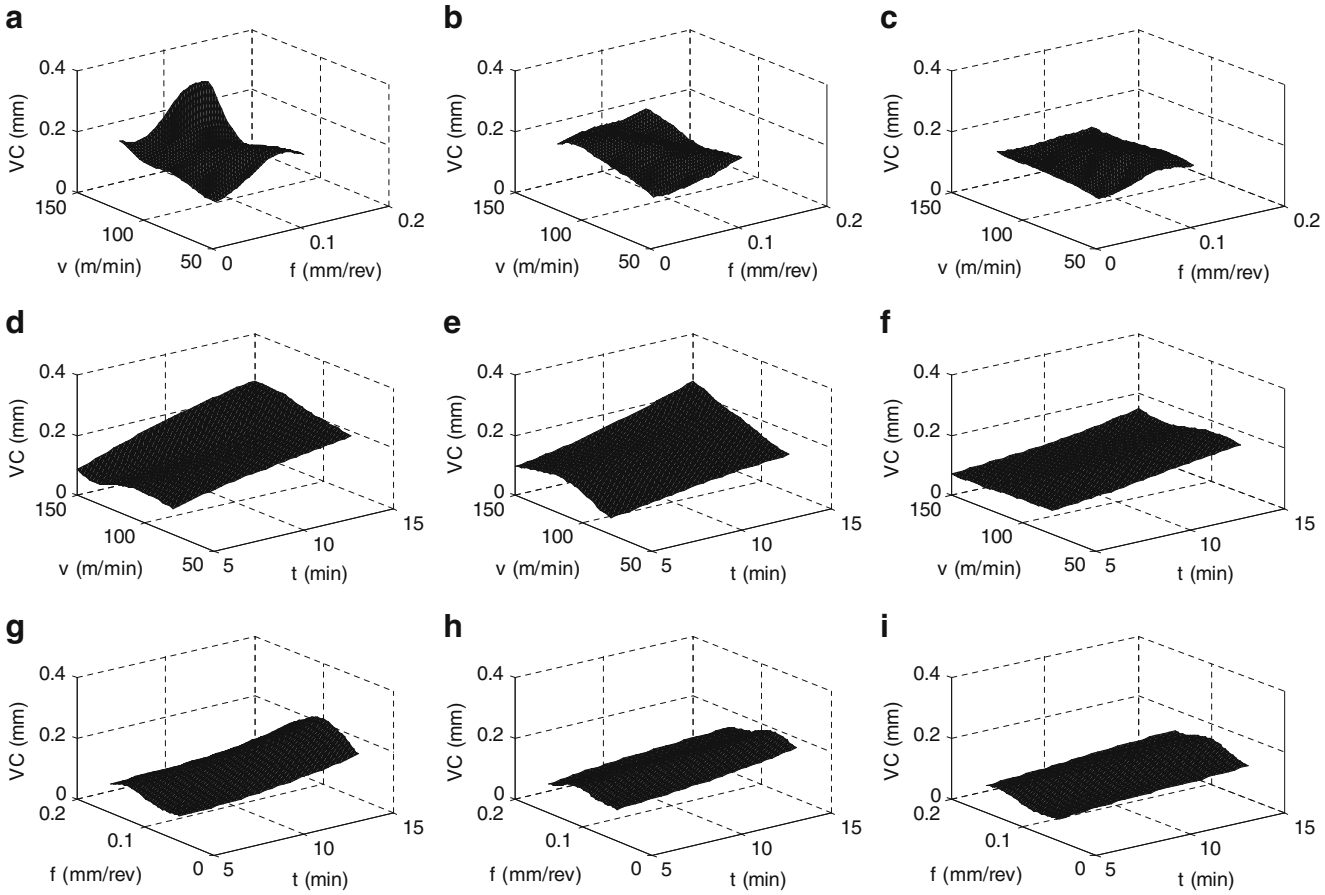

Fig. 12 Response surface *plots* showing the effect of two variables on tool wear: **a**–**c** cutting speed and feed rate; **d**–**f** cutting speed and machining time; **g**–**i** feed rate and machining time

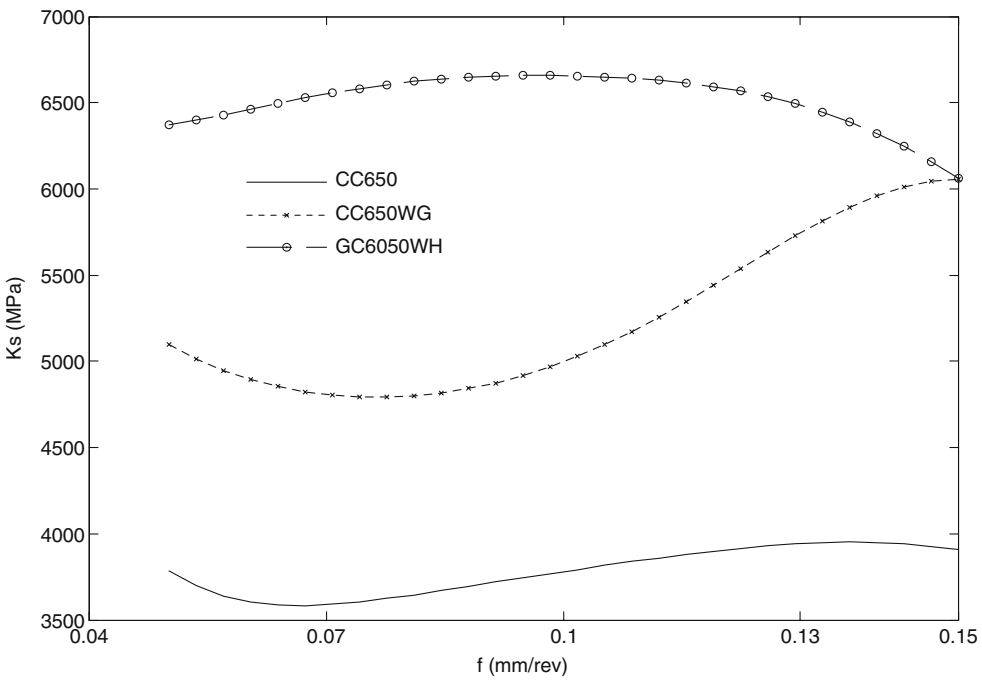

Fig. 13 Effect of feed rate on specific cutting force (cutting speed=85 m/min; machining time=5 min)

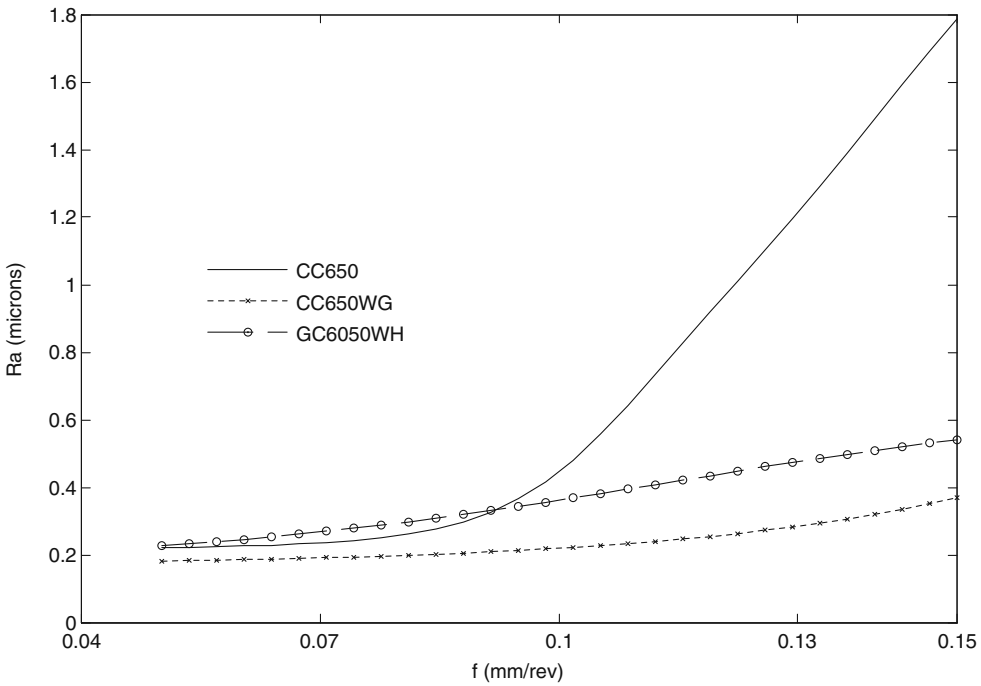

Fig. 14 Effect of feed rate on surface roughness (cutting speed=85 m/min; machining time=5 min)

superior as compared with CC650 and CC650WG inserts. On the other hand, wiper ceramic inserts (CC650WG and GC6050WH) perform better compared with conventional insert (CC650) from the viewpoint of surface roughness. Lower values of cutting speed and machining time are essential to minimize all the three machinability aspects. On the other hand, low feed rate is required to minimize the surface roughness and tool wear. However, this results in increased specific cutting force, and hence, a trade-off in feed rate becomes inevitable. Therefore, further investigation is still required for the selection of feed rate on machinability aspects. Hence, it has been decided to carry out the performance study on the machinability aspects for all the three ceramic inserts selected for varying feed rates at lower values cutting speed and machining time.

Figure 13 shows the comparison of specific cutting force for the three ceramic inserts as a function of feed rate variation. It is clear that the conventional insert CC650 is

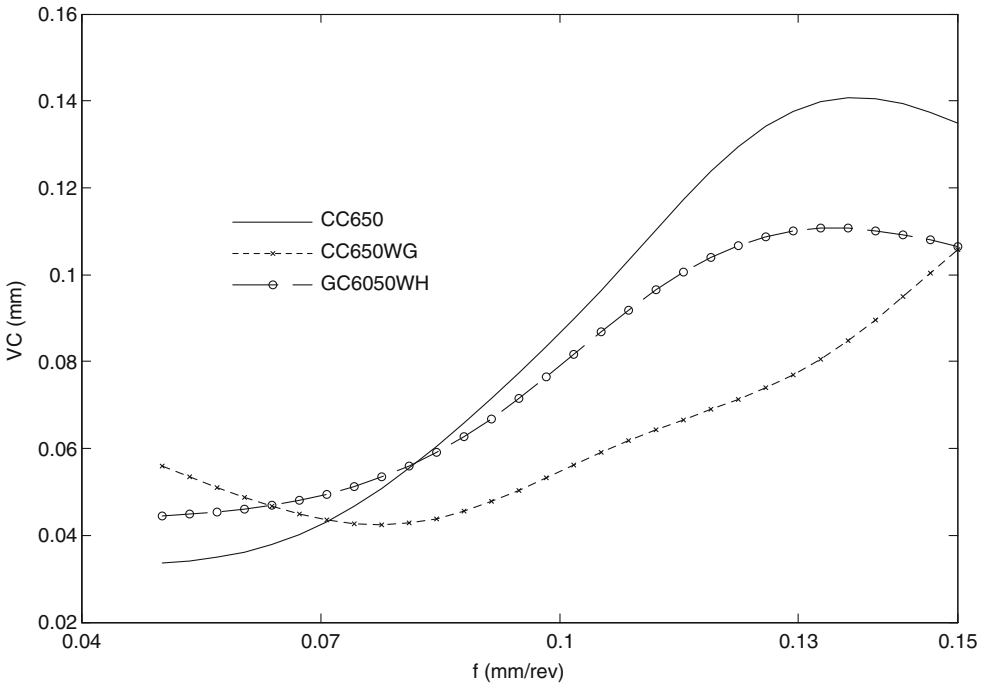

Fig. 15 Effect of feed rate on tool wear (cutting speed=85 m/min; machining time=5 min)

more desirable than the wiper inserts for all the feed rate values selected in the range 0.05–0.15 mm/rev. As seen from Fig. 14, the surface roughness is almost more or less same at low feed rate values below 0.09 mm/rev for all the three ceramic inserts. However, with conventional CC650 insert, the surface roughness sharply increases with the feed rate beyond 0.09 mm/rev. In such conditions, wiper ceramic inserts perform better as compared with conventional insert. Furthermore, the CC650WG results in minimum possible surface roughness as compared with GC6050WH at all feed rate values. Figure 15 demonstrates the variation of tool wear as a function of feed rate. It is seen that, for feed rate beyond 0.07 mm/rev, the tool wear increases with feed rate in all the three inserts tested. A comparison of tool wear reveals that the CC650WG insert is recommended from tool wear point of view. Hence, from the above comparison study, it can be concluded that CC650WG wiper ceramic insert results in minimum surface roughness and tool wear for the feed rate operating in the range medium-to-high. On the other hand, conventional insert is beneficial for minimizing the specific cutting force as compared with wiper ceramic inserts irrespective of the feed rate.

5 Conclusions

The ANN has been employed to analyze the effects of cutting speed, feed rate, and machining time on three aspects of machinability, namely, specific cutting force, surface roughness, and tool wear during hard turning of high chromium AISI D2 cold work tool steel. The performance of three different ceramic inserts, namely, conventional CC650 and wiper inserts of CC650WG and GC6050WH has been studied. A multilayer feed-forward ANN has been employed, which was trained by EBPTA. The input–output patterns required for training and testing of ANN models were obtained through the turning experiments planned through FFD. 3D response surface plots were generated to study the interaction effects of process parameters, and the following conclusions are drawn from the current investigation.

- The 3D response surface plots clearly indicate the existance of non-linear relationships between the process parameters and the machinability characterstics and thus justifying the use of ANN model.
- The specific cutting force is minimal at higher values of feed rate and lower values of cutting speed. The GC6050WH ceramic insert is found to be better as compared with CC650 and CC650WG inserts.
- The specific cutting force is also minimal for lower values of both cutting speed and machining time for all the three ceramic inserts. But, the specific cutting force is more in case of CC650WG when compared with others.
- For specified values of feed rate and machining time, the wiper GC6050WH ceramic insert results in lesser specific cutting force, which requires higher feed rate to minimize it.
- The wiper ceramic inserts (CC650WG and GC6050WH) are desirable for achieving a better surface finish as compared with conventional insert (CC650).
- Tool wear is highly sensitive to cutting speed and feed rate variations as compared with machining time for all the ceramic inserts. The GC6050WH wiper ceramic insert has an edge over the other for minimizing the tool wear.
- The comparison study reveals that the CC650 conventional insert is advantageous for minimizing the specific cutting force irrespective of the feed rate. On the other hand, CC650WG wiper ceramic insert is useful for minimizing both surface roughness and tool wear in medium-to-high range.

References

1. Konig W, Berktold A, Koch KF (1993) Turning versus grinding—a comparison of surface integrity aspects and attainable accuracies. Annals of CIRP 42(1):39–43
2. Tonshoff HK, Arendt C, Ben Amor R (2000) Cutting of hardened steel. Annals of CIRP 49(2):547–566
3. Zou JM, Anderson M, Stahl JE (2004) Identification of cutting errors in precision hard turning process. J Mater Process Technol 153–154:746–750
4. Rech J, Moisan A (2003) Surface Integrity in finish hard turning of case hardened steels. Int J Mach Tools Manuf 43:543–550
5. Destefani J (2004) Technology key to mold making success. Manuf Eng 133(4):59–64
6. Elbestawi MA, Chen L, Becze CE, EI-Wardany TI (1997) High-speed milling of dies and molds in their hardened state. Annals of CIRP 46(1):57–62
7. Byrne G, Dornfeld D, Denkena B (2003) Advancing cutting technology. Annals of CIRP 52(2):483–507
8. Klocke F, Brinskmeier E, Weinert K (2005) Capability profile of hard cutting and grinding processes. Annals of CIRP 54(2):557–580
9. GuoYB SJA (2004) Comparative study of hard turned and cylindrically ground white layers. Int J Mach Tools Manuf 44:135–145
10. Thiele JD, Melkote SN, Peascoe RA, Watkins TR (2000) Effect of cutting edge geometry and workpiece hardness on surface residual stresses in finish hard turning of AISI 52100 steel. ASME J Manuf Sci Eng 122:642–649
11. Huang Y, Liang SY (2003) Cutting forces modeling considering the effect of tool thermal property—application to CBN hard turning. Int J Mach Tools Manuf 43:307–315
12. ChouYK ECJ (1997) Tool wear mechanism in continuous cutting of hardened tool steels. Wear 212:59–65
13. Chou YK, Evans CJ, Barash MM (2002) Experimental investigation on CBN turning of hardened AISI 52100 steel. J Mater Process Technol 124:274–283

14. Thiele JD, Melkote SN (1999) Effect of cutting edge geometry and workpiece hardness on surface generation in the finish hard turning of AISI 52100 steel. J Mater Process Technol 94:216–226
15. Ozel T, Hsu T-K, Zeren E (2000) Effects of cutting edge geometry, workpiece hardness, feed rate and cutting speed on surface roughness and forces in finish turning of hardened AISI H13 steel. Int J Adv Manuf Technol 25(3–4):262–269
16. Kishawy HA, Elbestawi MA (2000) Tool wear and surface integrity during high-speed turning hardened steel with polycrystalline cubic boron nitride tools. J Eng Manuf 215:755–767
17. EI-Wardany TI, Kishawy HA, Elbestawi MA (2000) Surface integrity of die material in high-speed hard machining, part 1, micro graphical analysis. ASME J Manuf Sci Eng 122(4):620–631
18. EI-Wardany TI, Kishawy HA, Elbestawi MA (2000) Surface integrity of die material in high-speed hard machining, part 2, micro hardness variations and residual stresses. ASME J Manuf Sci Eng 122(4):632–641
19. Poulachon G, Bandyopadhyay BP, Jawahir IS, Pheulpin S, Seguin E (2003) The influence of the microstructure of hardened tool steel workpiece on the wear of PCBN cutting tools. Int J Mach Tools Manuf 43:139–144
20. Lima JG, Avila RF, Abrao AM, Faustino M, Davim JP (2005) Hard turning AISI 4340 high strength low alloy steel and AISI D2 cold work steel. J Mater Process Technol 169:388–395
21. Pavel R, Marinescu I, Deis M, Pillar J (2005) Effect of tool wear on surface finish for a case of continuous and interrupted hard turning. J Mater Process Technol 170:341–349
22. Diniz AE, Oliveira AJ (2008) Hard turning of interrupted surfaces using CBN tools. J Mater Process Technol 95:275–281
23. Chou YK, Song H (2004) Tool nose radius effects on finish turning. J Mater Process Technol 148:259–268
24. Kumar AS, Durai R, Sornakumar T (2003) Machinability of hardened steel using alumina based ceramic cutting tools. Int J Refract Met Hard Mater 21:109–117
25. Benga GC, Abrao AM (2003) Turning of hardened 100Cr6 bearing steel with ceramic and PCBN cutting tools. J Mater Process Technol 143–144:237–241
26. Grzesik W, Wanat T (2005) Comparative assessment of surface roughness produced by hard machining with mixed ceramic tools including 2D and 3D analysis. J Mater Process Technol 169:364–371
27. Grzesik W, Wanat T (2006) Hard turning of quenched alloy steel parts using conventional and wiper ceramic inserts. Int J Mach Tools Manuf 46:1988–1995
28. Grzesik W (2008) Influence of tool wear on surface roughness in hard turning using differently shaped ceramic tools. Wear 265:327–335
29. Schwach DW, Guo YB (2005) Feasibility of producing optimal surface integrity by process design in hard turning. Mater Sci Eng 395:116–123
30. Quiza R, Figueira L, Davim JP (2008) Comparing statistical models and artificial networks on predicting the tool wear in hard machining D2 AISI steel. Int J Adv Manuf Technol 37:641–648
31. Ozel T, Karpat Y (2005) Predictive modeling of surface roughness and tool wear in hard turning using regression and neural networks. Int J Mach Tools Manuf 4:467–479
32. Davim JP, Figueira L (2007) Machinability evaluation in hard turning of cold work tool steel (D2) with ceramic tools using statistical techniques. Mater Des 28:1186–1191
33. Klocke F, Kratz H (2005) Advanced tool edge geometry for high precision hard turning. Annals of CIRP 54(1):47–50
34. Ozel T, Karpat Y, Figueira L, Davim JP (2007) Modelling of surface finish and tool flank wear in turning of AISI D2 steel with ceramic wiper inserts. J Mater Process Technol 189:192–198
35. Davim JP, Figueira L (2007) Comparative evaluation of conventional and wiper ceramic tools on cutting forces, surface roughness and tool wear in hard turning AISI D2 steel. J Eng Manuf 221:625–633
36. Gaitonde VN, Karnik SR, Figueira L, Davim JP (2009) Machinability investigations in hard turning of AISI D2 cold work tool steel with conventional and wiper ceramic inserts. Int J Refract Met Hard Mater 27(4):754–763
37. Montgomery DC (2004) Design and analysis of experiments, 5th edn. Wiley, New York
38. Karnik SR, Gaitonde VN, Davim JP (2008) A Comparative study of the ANN and RSM modeling approaches for predicting burr size in drilling. Int J Adv Manuf Technol 38:868–883
39. Karnik SR, Gaitonde VN, Mata F, Davim JP (2008) Investigative study on machinability aspects of unreinforced and reinforced PEEK composite machining using ANN model. J Reinf Plast Compos 27(7):751–768
40. Karnik SR, Gaitonde VN, Rubio JC, Correia AE, Abrao AM, Davim JP (2008) Delamination analysis in high speed drilling of carbon fiber reinforced plastics (CFRP) using artificial neural network model. Mater Des 29:1768–1776
41. Davim JP, Gaitonde VN, Karnik SR (2008) Investigations into the effect of cutting conditions on surface roughness in turning of free machining steel by ANN models. J Mater Process Technol 205:16–23
42. Schalkoff RB (1997) Artificial neural networks. McGraw-Hill, Singapore
43. Fausett L (1994) Fundamentals of neural networks: architectures, algorithms and applications. Prentice–Hall, New York
44. Math Works Incorporation (2005) MATLAB User Manual, Version 7.1, R 14. Natick, MA